

Preparation and Characterization of Surface-Functionalized Polysilsesquioxane Hard Spheres in Aqueous Medium

Subramani Sankaraiah

Department of Chemistry, Missouri University of Science and Technology, Rolla, Missouri 65409-0010

Jung Min Lee and Jung Hyun Kim*

Department of Chemical and Biomolecular Engineering, Yonsei University,
134 Shinchon-Dong, Seodaemun-Gu, Seoul 120-749, Republic of Korea

Sung Wook Choi

Department of Biomedical Engineering, Washington University in St. Louis,
St. Louis, Missouri 63130-4899

Received February 14, 2008; Revised Manuscript Received June 22, 2008

ABSTRACT: Nanosized silica and functionalized silica spherical particles have typically been made by complex methods, which were then used as template materials to fabricate nanostructured materials. However, in a simple one-step hydrolytic co-condensation process, we synthesized various sizes of nano/micro hard spheres of functionalized network polysilsesquioxanes, similar to functionalized silica, of narrow size distribution from heterogeneous mixtures of organomethoxysilanes, surfactants, water, and ammonium hydroxide solution. The size of the spherical polysilsesquioxanes particles could be controlled from nanometer to micrometer by adjusting and changing the organomethoxysilane composition, the molar ratio, and the catalyst concentration. The resulting monodisperse particles possessed surface organic functional groups having similar properties and applications as found in functionalized silica spherical particles. The functional polysilsesquioxane spherical particles were characterized by scanning electron microscopy and dynamic light scattering to elucidate the particles' morphologies. The compositions of the polysilsesquioxanes were confirmed by FT-IR spectroscopy, solid-state NMR spectroscopy, differential scanning calorimetry, thermogravimetric analysis, and elemental analysis.

Introduction

Recently, there has been considerable interest in the development of organic–inorganic hybrid materials in the chemistry and physics fields. In the development of these materials, organically modified silicas or ormosils and silsesquioxanes (where the general formula is $[R_2Si_2O_3]_n$ and R is an organic group or hydrogen) are mostly used.^{1–5} The well-established hydrolytic sol–gel route which involves base- or acid-catalyzed hydrolysis and condensation reactions of monomeric alkoxy-silane precursors in an aqueous solvent system are widely used to prepare these materials.⁶ For the synthesis of ormosil particles, the most common approach has involved grafting of organic groups by chemical reaction of presynthesized Stober silica particles with certain silane coupling agents.^{7,8} Another approach involves the Stober synthesis of ormosil particles starting from mixtures of tetraalkoxysilane (TAOS) and organotrialkoxysilane precursors with the general formula $RSi(OR')_3$, where R = methyl, vinyl, phenyl, octyl, mercaptopropyl, or aminopropyl and R' = methyl or ethyl.^{7,9–14} These silica-based particles were generated by co-condensation of tetraalkoxysilane–organoalkoxysilane droplets in water.

Preparation of organosilicas, however, always requires two or more complex processing steps and is difficult to obtain a high yield of monodisperse particles. Hence, the preparation of improved functional polysilsesquioxanes (FPSQs) by one-step hydrolytic co-condensation of a mixture of organoalkoxysilanes is valuable. FPSQs having a variety of functional groups including mercapto, epoxy, amine, vinyl, acrylic, isocyanate, and other organic groups are among the most interesting

materials for preparing hard spheres of narrow size distribution. These extremely tailorable materials are interesting because organoalkoxysilanes can be easily hydrolyzed or cohydrolyzed and condensed into spherical particles of narrow size distribution. Polysilsesquioxanes (PSQs) possess two unique structural features: (1) the chemical composition is a hybrid that is intermediate ($RSiO_{1.5}$) between that of silica (SiO_2) and silicones (R_2SiO); (2) PSQ molecules are nanoscopic in size. These materials are thermally and chemically more robust than silicones, and their nanostructured shape and size provide unique properties by controlling polymer chain motion at the molecular level.

The syntheses of FPSQs are attracting increasing attention due to the potential applicability of these materials in a wide range of technologies.^{15–19} A simple sol–gel process has been reported for the preparation of ormosil nanoparticles with diameters in the range 60–180 nm directly from organotrialkoxysilane precursors in the absence of a surfactant using excess alcohol.²⁰ In another report, a remodeled sol–gel process was used to make particles larger than 1 μm using a single monomer of mercapto- or vinyltrialkoxysilane.²¹ It has also been reported the preparation of poly(vinylsilsesquioxane) from vinyltrimethoxysilane (VTMS) and poly(3-mercaptopropylsilsesquioxane) from 3-mercaptopropyltrimethoxysilane (MPTMS).¹⁶ In these reports, a single organoalkoxysilane monomer was used to produce vinyl- or mercapto-functional polysilsesquioxane particles. In the literature, there appear to be no reports about the preparation of cohydrolyzed (copolymerized) FPSQ nano/micro particles. Hence, we report in this paper, for the first time, a simple, reproductive one-step synthetic process for synthesizing copolymerized FPSQ nano/micro hard spheres in

* Corresponding author: Tel +82 2 2123 7633; Fax +82 2 312 0305; e-mail jayhkim@yonsei.ac.kr.

an aqueous medium using methyltrimethoxysilane (MTMS) as a precursor.

Copolymerized FPSQ nano and micro particles having various functional groups were obtained by hydrolytic co-condensation of MTMS with functional organomethoxysilanes in the presence of the aqueous ammonium hydroxide catalyst. The key reaction parameters responsible for the control of size and morphology of the particles can be effectively controlled by changing the reaction conditions such as the concentration of catalyst and organoalkoxysilanes ratio. The copolymerized FPSQ particles were characterized in view of the morphological observation and the structural investigation. If the organic functional groups introduced are reactive, its structural and chemical properties can be further tailored.²² Since the Si–C bond in organoalkoxysilane is stable with respect to hydrolysis, a variety of modifications can be directly and durably incorporated into the network, depending on the nature of the organofunctional silane precursor.

Experimental Section

Materials. The organosilanes, methyltrimethoxysilane (MTMS), 3-mercaptopropyltrimethoxysilane (MPTMS), 3-methacryloxypropyltrimethoxysilane (MAPTMS), vinyltrimethoxysilane (VTMS), 3-aminopropyltrimethoxysilane (APTMS), phenyltrimethoxysilane (PTMS) and hydrogen tetrachloroaurate(III) trihydrate used in this work were purchased from Aldrich Chemicals. The surfactant and stabilizer used were disodium laurylphenol ether disulfonate (anionic surfactant, Dow Chemical Co.) and polyvinylpyrrolidone (PVP, MW 40 000, polymeric stabilizer, Fluka Chemicals), respectively. Ammonium hydroxide solution (NH₄OH, 28%) was purchased from Wako Pure Chemical Co. All chemicals used in these experiments were used as received without further purification. DDI water obtained from a Milli-Q water purification system (Millipore) was used for hydrolysis and condensation of organomethoxysilanes.

Synthesis of FPSQs by Hydrolytic Co-condensation Process. The following synthesis procedure was typically used. In the typical preparation of cohydrolyzate of the organomethoxysilanes, the required amount of surfactant and PVP were dissolved in 25 mL of well-cooled water. A required amount of ammonium hydroxide (28%) solution was added into the aqueous medium, and the temperature of the medium was kept at 15–20 °C. An organomethoxysilane mixture was added gradually to the aqueous medium for about 1 h at the same temperature (15–20 °C). The reaction was continued overnight at room temperature. Finally, the particles were separated from the aqueous mixture by centrifugal sedimentation to remove surfactants and redispersed in water. The reaction product consisted of FPSQ resin particles in water. The resin particles were observed to be of narrow size distribution with particle size in the range 0.05–5 μ m.

The particle size was controlled and studied by changing surfactant concentration, ammonium hydroxide concentration, and organomethoxysilane ratio. The effect of the amount of catalyst on the spherical particles was thoroughly examined at the fixed molar ratio between organomethoxysilane and water. In these modified sol–gel process experiments, methanol or ethanol was not used for the formation of the spherical resin particles. The compositions of FPSQs prepared are presented in Table 1.

Preparation of MP-PSQ/Metal Conductive Microparticles. Approximately 0.1 g of 10 wt % MP-PSQ microparticles (MP-PSQ6) was mixed and stirred at 70 °C for 24 h with 100 mL of hydrogen tetrachloroaurate(III) trihydrate (0.125 \times 10^{−3} M) aqueous solutions. The metal-functionalized MP-PSQ particles settled to the bottom of the reaction vessel. The MP-PSQ–metal composite particles were recovered by centrifugation and copiously washed with water and ethanol prior to microscopic studies.¹⁶

Characterization. Elemental analyses were performed with an EA1110 (CE Instrument, Italy) elemental analyzer. The operating condition of the elements followed the TCD CHNS PoraPak POS column 600 s analysis time; 50–190 °C temperature range. FT-IR spectra were recorded on a Bruker Tensor 27 FT-IR spectrophoto-

Table 1. Composition (in grams) of FPSQs^a

materials	MTMS	MPTMS	MAPTMS	VTMS	APTMS	PTMS	catalyst ^c (28%)
M-PSQ1	9.30						0.005
M-PSQ2	9.30						0.040
M-PSQ3 ^b	9.30						0.040
MP-PSQ1	9.30	0.24					0.040
MP-PSQ2	9.30	0.24					0.005
MP-PSQ3	9.30	0.24					0.010
MP-PSQ4	9.30	0.24					0.015
MP-PSQ5	9.30	0.24					0.020
MP-PSQ6	9.06	0.48					0.005
MP-PSQ7	8.50	1.04					0.005
MA-PSQ1	9.75		0.25				0.040
MA-PSQ2	9.30		0.24				0.010
MA-PSQ3	9.06		0.48				0.010
V-PSQ1	9.50			0.50			0.040
V-PSQ2	9.06			0.48			0.005
A-PSQ1	9.75				0.25		0.040
A-PSQ2	9.30				0.24		0.005
P-PSQ1	9.00					1.00	0.040
P-PSQ2	9.06					0.48	0.005

^a In all experiments except M-PSA3, the amount of water, disodium laurylphenol ether disulfonate, and PVP amount used were 25, 0.2, and 0.02 g, respectively. PSQ = polysilsesquioxanes, M = methyl, MP = mercaptopropyl, MA = methacryloxypropyl, V = vinyl, A = aminopropyl, P = phenyl. ^b Water: 25 g; disodium laurylphenol ether disulfonate: 0.1 g; PVP: 0.01 g. ^c Catalyst (28% ammonium hydroxide).

meter (Bruker Optics, Germany). The samples were mixed with potassium bromide and pressed to a disk to measure the absorption spectrum. The measurements were carried out over the 4000–400 cm^{−1} range. The number of scans per spectrum was 32, and the spectral resolution was 4 cm^{−1}. High-resolution solid-state NMR spectra were measured at room temperature on a Bruker Avance II 500 MHz spectrometer (silicon frequency 99.36 MHz, carbon 125.75 MHz) equipped with a Bruker solid-state accessory. Spectra were obtained using a broadband probehead with a 4 mm double air bearing magic-angle spinning assembly. Spinning speeds of ~5 kHz were employed. The 90° pulse lengths for the nuclei ¹³C and ²⁹Si were ~2.9 μ s. Cross-polarization (CP) contact time was between 0.5 and 5 μ s for carbon and 0.5 and 3 μ s for silicon. The delay time between pulses in the CP experiments were 5 s for carbon and 10 s for silicon. Chemical shifts of silicon atoms in silsesquioxane compounds are referred to using the traditional terminology *Tⁿ*, where the superscript corresponds to the number of oxygen bridges to other silicon atoms. Thus, an uncondensed monomer was designated *T⁰* and a fully condensed polymer with no residual silanols was assigned as *T³* silicon atoms.

The particle size of the FPSQ dispersion particles was measured using a Zetasizer 3000HSA (Malvern Inst. Ltd., UK). A FE-SEM (JEOL JSM6500F field emission SEM, Tokyo, Japan) was utilized to study the FPSQ particles diameter and the morphology. The particles from a diluted aqueous dispersion were deposited onto a silicon wafer at room temperature. They were dried under vacuum and sputter-coated with gold for SEM observations. The average diameter and standard deviation were determined from SEM images by averaging diameters of over ca. 100 particles. TGA was performed on a TA Instruments TGA-Q50 thermal analyzer under flowing nitrogen at a heating rate of 10 °C min^{−1}. Differential scanning calorimeter (DSC), TA Instruments model DSC Q10, was used to examine the thermal behavior of FPSQs with a heating rate of 10 °C min^{−1} under nitrogen purge of 30 mL min^{−1}. Surface area data were performed on a Micromeritics ASAP 2020 surface area and porosity analyzer with BET method after the samples were outgassed for 24 h at 75 °C. Total surface areas (*S_t*) were measured using the BET method. Specific surface areas (*S_{BET}*) were calculated by dividing *S_t* by the sample weight. Total pore volumes (*V_p*) were obtained at a relative pressure of 1.00. The % porosity (ϕ) and average pore diameters (*D*) were obtained using the following formulas:

$$\varphi = V_p / (V_p + 0.455) \times 100$$

$$D = (4V_p / S_{\text{BET}}) \times 900$$

Results and Discussion

FPSQs Syntheses. Syntheses of FPSQ particles with controllable amount of methyl, mercaptopropyl, methacryloxypropyl, vinyl, aminopropyl, and phenyl functional groups using MTMS as a main precursor by hydrolytic co-condensation process were conducted. This approach was capable of producing nano/micro particles of various particle diameters with narrow size distribution. No silica seed particles were necessary as nucleation sites and the particle formation of FPSQs were well-controlled in the presence of surfactant by base catalyst and organotrimethoxysilane ratios. The effects of the catalyst concentration and organotrimethoxysilane ratios on the particle size have been studied in order to develop a procedure that is best suited to the production of a wide range of monodisperse nano/micro FPSQ particles.

In order to understand the basic mechanism of particle formation, many experiments were conducted by changing the surfactant, catalyst concentrations, and methoxysilane ratios, and the obtained selected results are listed in Tables 1 and 2. In these experiments, MTMS was chosen and used as main precursor and hydrolyzed at various concentrations of catalyst and surfactant. The morphologies of the nano/micro M-PSQ particles prepared using MTMS monomer alone were examined by SEM and are shown in Figure 1.

When the amount of NH_4OH was 0.04 g, nanoparticles of 15.9% polydispersity were obtained with a diameter of ~ 79 nm (M-PSQ2). A decrease in the surfactant amount (M-PSQ3) and the concentration of NH_4OH to 0.005 g (M-PSQ1) resulted in microparticles of 1.3 and 2.6 μm diameter and 13% and 14.6% polydispersity, respectively. It is clear from these images that the M-PSQ particles were spherical in shape, of micrometer size and mostly monodisperse. Particle size was increased with a decreasing surfactant concentration, while the particle size distribution was also markedly affected by surfactant concentration.

The effect of surfactant concentration on the particle size was explained as follows. The average particle size decreased with an increase in the surface tension (i.e., a decrease in the surface activation) of the emulsifier, which reflects the relatively greater number of hydrophilic groups in methylsilsesquioxane polymer compared with hydrophobic groups. Since the surface of methylsilsesquioxane particles is covered by methyl groups, the resulting methylsilsesquioxane colloid is considered to be labile in water. The use of emulsifiers is therefore believed to stabilize the colloid. In these experiments, the particle sizes are systematically controlled by adjusting the concentration of the NH_4OH , in the presence of MTMS precursor.¹⁶

Generally, hydrolytic condensation of the organotrimethoxysilanes in water or ethanol–water was quite rapid under basic conditions.^{23–25} Initial hydrolysis of the organotrimethoxysilanes resulted in silanol functional oligomers. These Si–OH functions were very reactive and then condensed to form silsesquioxanes in the presence of base catalyst. During hydrolytic co-condensation reaction at higher catalyst concentration, white or transparent emulsions were obtained for all organotrimethoxysilane mixtures, while white precipitates appeared for all organotrimethoxysilane mixtures except MTMS/APTMS mixture at lower catalyst concentration. The hydrolysis products of MTMS/APTMS mixtures (unlike other organotrialkoxysilanes) were not precipitated from the solution even after 12 months but depended on the variation of MTMS/APTMS molar ratios. The reason for this result should be due to the strong interaction of amino groups with water molecules in aqueous medium. The excellent stability or solubility of co-condensed A-PSQs in water is also

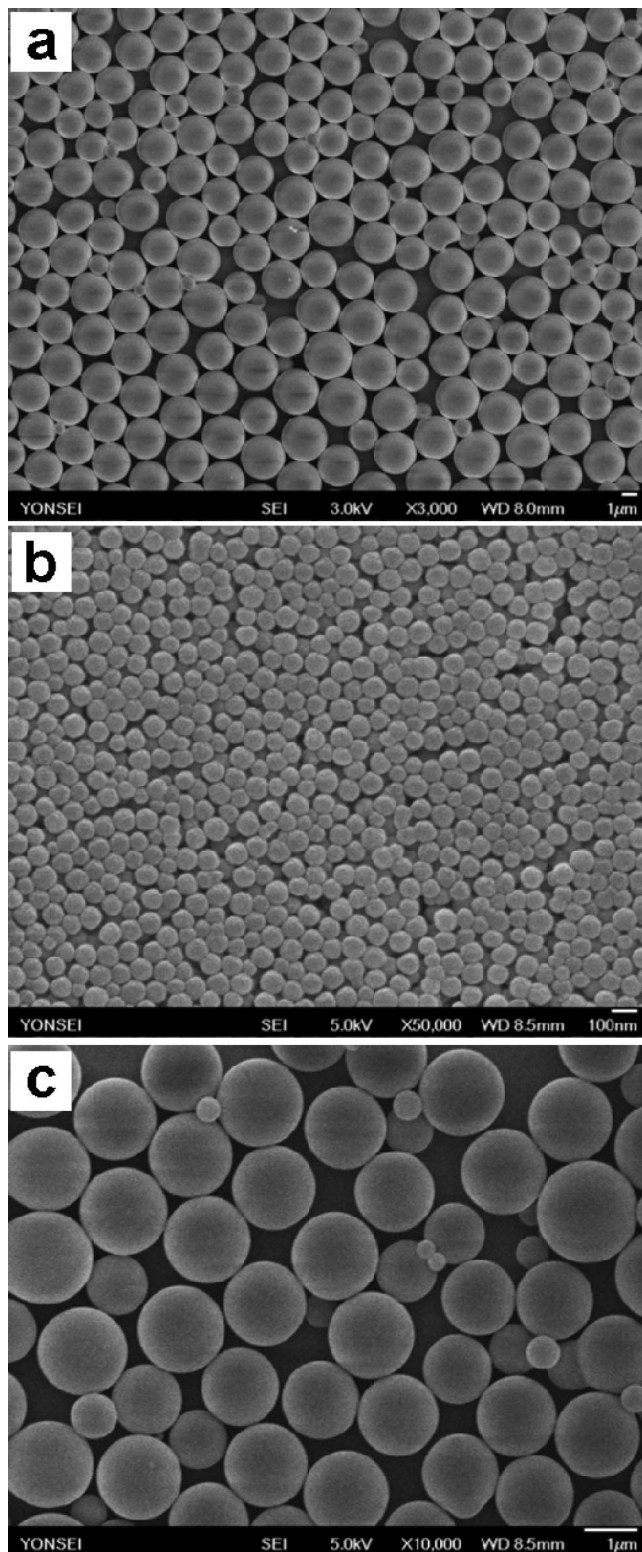


Figure 1. SEM images of MTMS based silsesquioxanes: (a) M-PSQ1, (b) M-PSQ2, and (c) M-PSQ3.

due to presence of highly water-soluble polar amino groups on the surface of the particles.¹⁷ However, it is clear that other organotrimethoxysilanes are water insoluble or immiscible, which result in white emulsions or precipitates due to the absence of highly polar organofunctional groups on the surface of the FPSQ particles.

From these basic experiments and the results, some of the factors responsible for control of particle morphology were

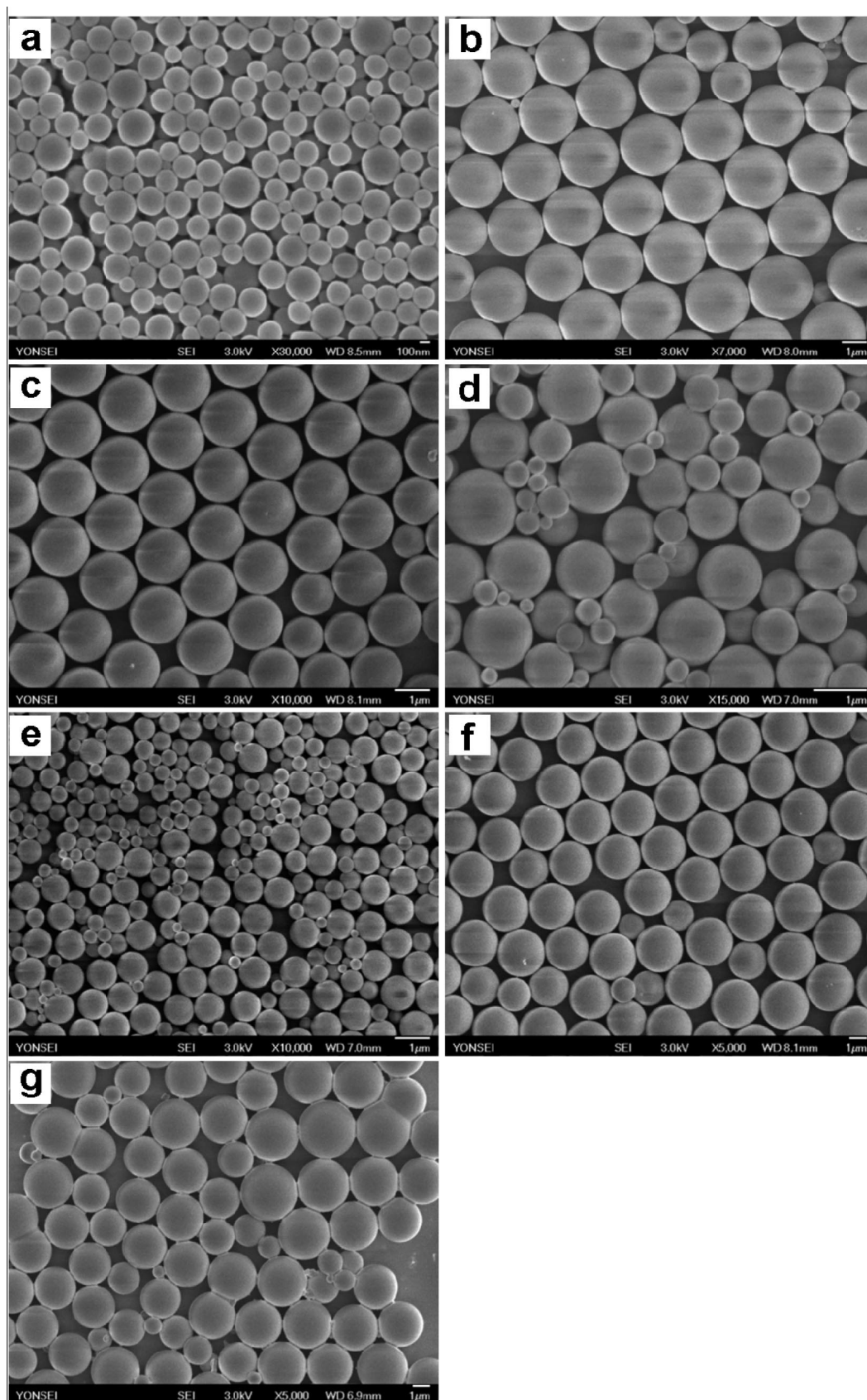


Figure 2. SEM images of MTMS/MPTMS-based silsesquioxanes: (a) MP-PSQ1, (b) MP-PSQ2, (c) MP-PSQ3, (d) MP-PSQ4, (e) MP-PSQ5, (f) MP-PSQ6, and (g) MP-PSQ7.

elucidated to investigate the boundaries of the types of particulate product accessible via cohydrolysis of alkoxy silane mixtures with functional groups. In these studies, MP-PSQ particles were prepared by cohydrolysis of MTMS/MPTMS at

various catalyst concentration levels (0.005, 0.010, 0.015, 0.02, and 0.04 g of 28% NH_4OH) at a constant MTMS/MPTMS ratio (9.3:0.24) and changing the MTMS/MPTMS ratio at a constant catalyst concentration.

Table 2. Average Particle Diameter, Polydispersity Index, and Polydispersity of FPSQs

materials	DLS		SEM	
	av particle size (μm)	PDI ^a	av particle size ^b (μm)	polydispersity ^c (%)
M-PSQ1			2.60	13.0
M-PSQ2	0.10	2.02	0.079	15.9
M-PSQ3			1.30	14.6
MP-PSQ1	0.20	2.65	0.212	25.6
MP-PSQ2			2.51	5.4
MP-PSQ3			1.58	7.6
MP-PSQ4	1.00	2.08	1.18	16.7
MP-PSQ5	0.90	2.30	0.81	20.1
MP-PSQ6			2.40	7.7
MP-PSQ7			2.29	11.3
MA-PSQ1	0.10	1.88	0.121	13.6
MA-PSQ2	0.80	2.24	1.17	19.2
MA-PSQ3			2.09	11.4
V-PSQ1	0.10	1.67	0.096	10.4
V-PSQ2	1.40	1.44	1.57	6.9
A-PSQ1	0.10	1.66	0.095	10.3
A-PSQ2	0.15	1.68	0.134	10.5
P-PSQ1	0.10	2.26	0.088	19.5
P-PSQ2			1.52	20.0

^a Polydispersity index, $\text{PDI} = \bar{D}_w/\bar{D}_n$, where \bar{D}_w and \bar{D}_n are weight- and number-average diameter of particles, respectively. ^b Averaged over ca. 100 particles. ^c Polydispersity (%) = (standard deviation/mean size) \times 100.

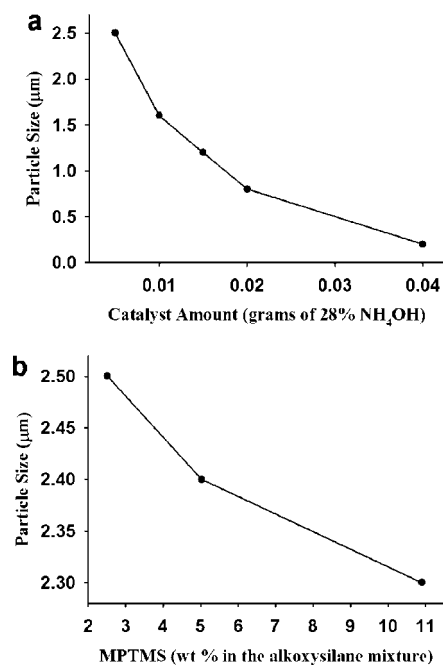


Figure 3. Particle sizes of FPSQ particles against (a) the amount of catalyst at a fixed ratio of MTMS/MPTMS and (b) the percentage of MPTMS in the MTMS/MPTMS mixture at a fixed catalyst amount.

The morphologies of the nano/micro MP-PSQ particles prepared using MTMS/MPTMS mixture examined by SEM are shown in Figure 2, and particle sizes and polydispersity (%) are given in Table 2. It can be seen from Figure 2 that the MP-PSQ particles are generally spherical in shape, with a smooth surface, where the diameter of the particles decreased and polydispersity (%) increased with an increase in catalyst concentration. Interestingly, the size of the particles also decreased slightly and polydispersity (%) increased with increasing MPTMS content in the MTMS/MPTMS mixture. The same trend was also expected in DLS data. The diameter of the spherical particles made using various catalyst concentration levels (0.005, 0.010, 0.015, 0.02, and 0.04 g of 28% NH_4OH) ranged from 2.51 to 0.2 μm , depending on the amount of catalyst

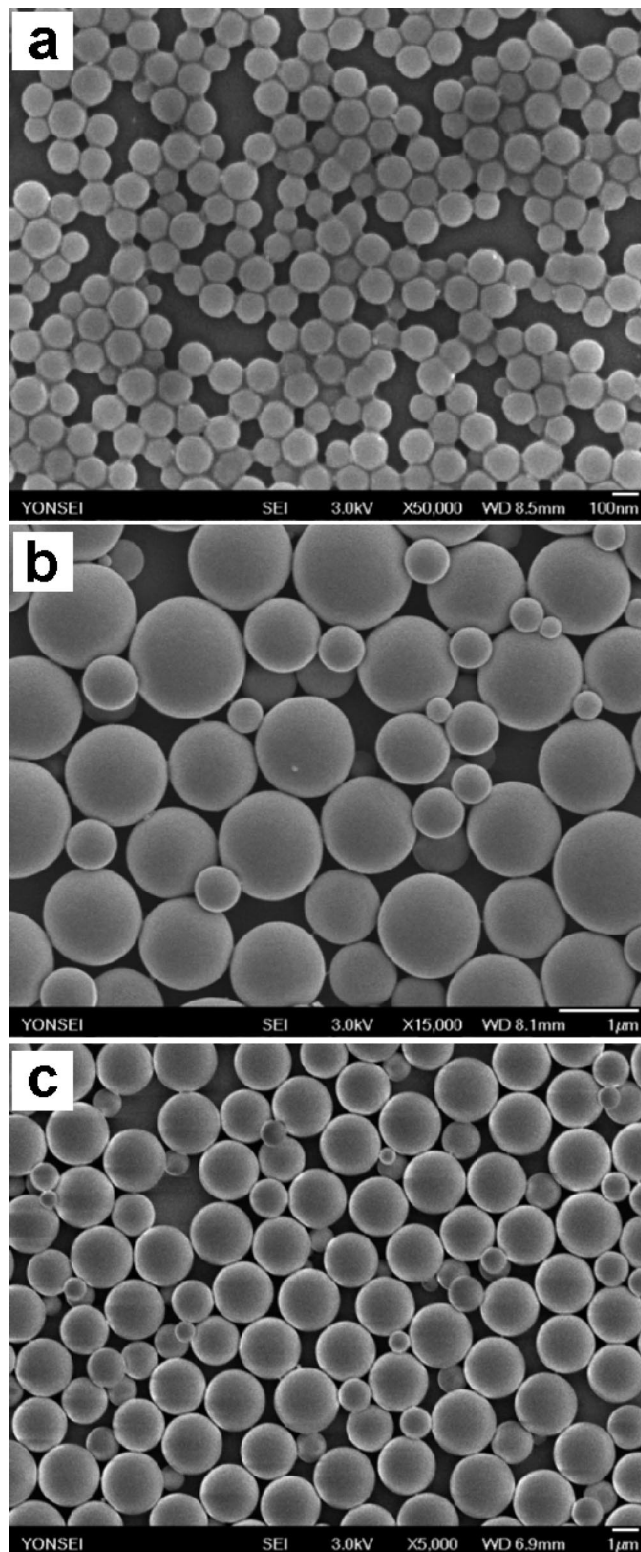


Figure 4. SEM images of MTMS/MAPTMS-based silsesquioxanes: (a) MA-PSQ1, (b) MA-PSQ2, and (c) MA-PSQ3.

used, while the particle size was 2.51–2.29 μm when MPTMS amount in the MTMS/MPTMS mixture increases (see Table 2). The effects of catalyst concentration and MPTMS amount on the particle sizes are presented in Figure 3. In general, products obtained using at low catalyst concentration were larger than those made at higher levels. Increase in hydrolysis rates with increasing ammonia concentration led to a higher nucleation rate, which also resulted in a larger number of particles though of smaller size.

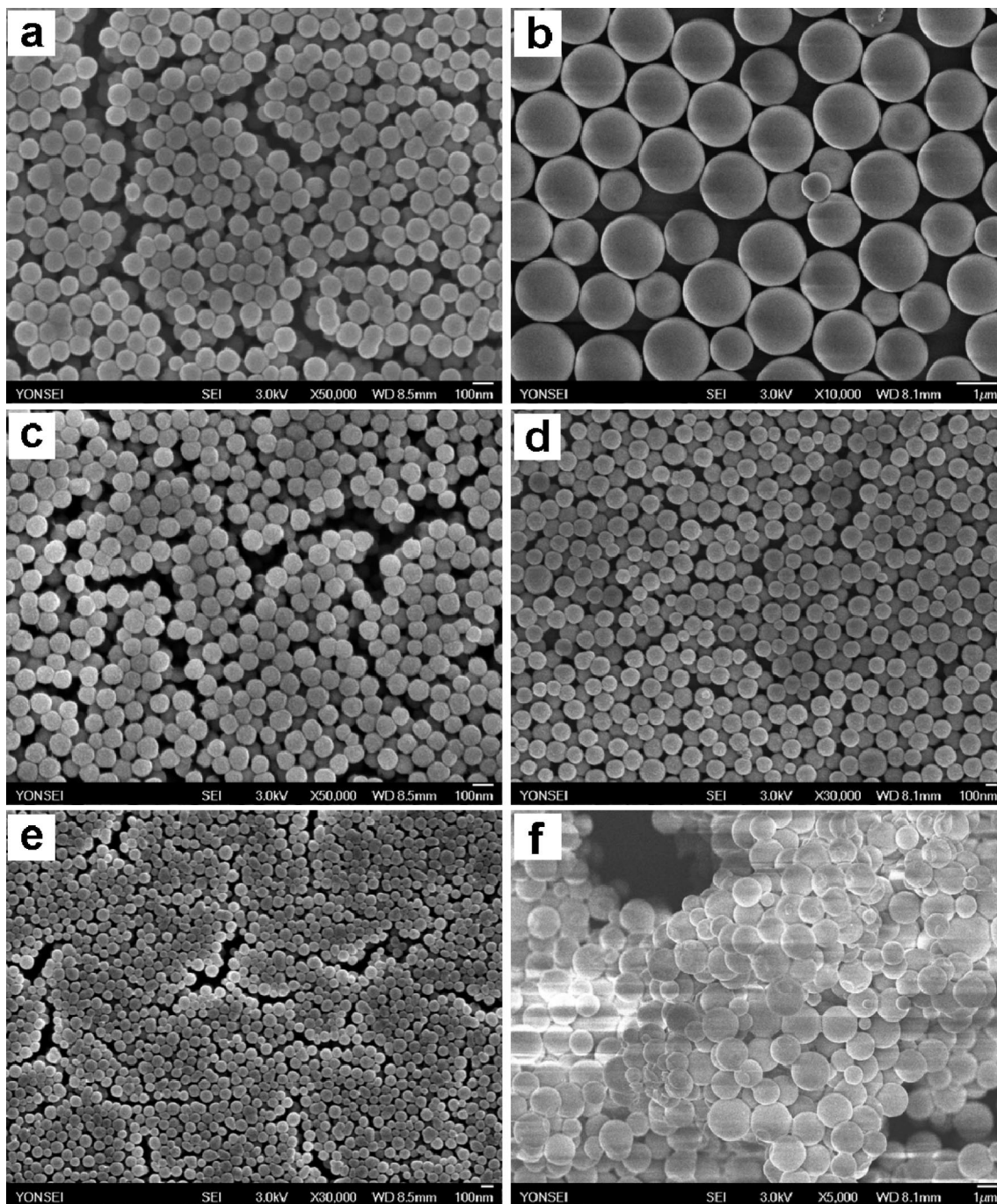


Figure 5. SEM images of different FPSQs: (a) V-PSQ1, (b) V-PSQ2, (c) A-PSQ1, (d) A-PSQ2, (e) P-PSQ1, and (f) P-PSQ2.

Table 3. Elemental Analysis and Weight Loss by TGA of FPSQs

material	calculated (wt %)				experimental (wt %)				temp (°C) at various % weight loss		
	C	H	N	S	C	H	N	S	5%	10%	15%
M-PSQ1	17.90	4.51			16.08	4.82			440	608	665
MP-PSQ6	18.58	4.57		1.64	16.32	5.02		1.67	390	553	661
MA-PSQ3	19.99	4.63			19.24	5.07			424	506	622
V-PSQ2	18.57	4.47			18.53	4.91			463	592	738
A-PSQ2	18.36	4.59	0.40		20.24	4.90	0.50		501	528	548
P-PSQ2	20.38	4.47			17.70	4.84					

In the case of MTMS/MAPTMS mixtures, it was seen that the size of the particles decreased with increasing ammonia concentrations, while it increased with increasing MAPTMS amount in the MTMS/MAPTMS mixtures, as seen in Figure 4. The same results were observed by DLS analysis (see Table 2). As the concentration of MAPTMS was altered from 0.24 to 0.48 g, the particle diameter showed a noticeable change from

1.17 to 2.09 μm , respectively, at same catalyst concentration level (see Table 2 and Figure 4).

Additional experiments were performed to understand the control of particle size of cohydrolyzate of VTMS, APTMS, and PTMS with MTMS precursor. These experiments were conducted under the same experimental conditions as like other experiments, at low and high catalyst concentration levels. As

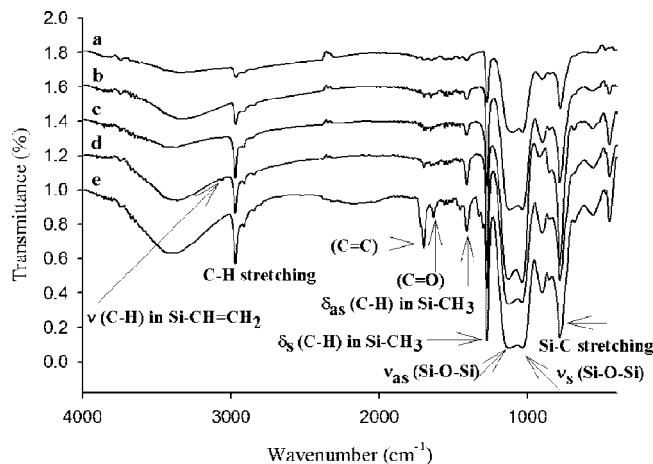


Figure 6. FT-IR spectra of FPSQs: (a) M-PSQ1, (b) MP-PSQ6, (c) A-PSQ2, (d) V-PSQ2, and (e) MA-PSQ3.

shown in Figure 5b, the particles obtained from MTMS/VTMS mixtures were uniform in diameter with 6.9% polydispersity. The particle sizes obtained at low and high catalyst concentrations were 0.096 and 1.57 μm , respectively. On the other hand, the particles prepared from MTMS/APTMS mixtures at low and high catalyst concentrations were mostly nanoparticles and sizes were in the range 0.095–0.15 μm , as seen in Figures 5c,d. As mentioned previously, A-PSQ nanoparticle formation at low and high catalyst concentrations could be due to the solubility behavior of resultant particles. Additionally, it is worth mentioning that the amino groups of APTMS (through raised pH) may catalyze to result in A-PSQ nanoparticles. Figures 5e,f represent the SEM images of P-PSQ particles made using MTMS/PTMS mixtures. The DLS data and SEM images confirmed that high catalyst concentration result in microparticles whereas nanoparticles result for low catalyst concentration.

As for the effect of the cohydrolysis on the size of the FPSQ particles, the results show some specific dependence on the bulk of the organic functional groups as shown in Table 2. Both electronic and steric factors likely play a role in determining the particle size when different organic groups are present. The nanoparticles obtained by cohydrolysis of MTMS/APTMS mixture could be due to the excellent solubility of APTMS in water, which makes nanosized, hydrolyzed particles to be more hydrophilic. The other organic functional alkoxyisilanes except APTMS resulted in FPSQ microparticles at low catalyst concentration.

The important factor for the formation of microparticles functionalized by organosilanes is hydrophobic nature of alkoxyisilanes, which results in hydrophobic particles. Because of the different chemical properties of ethoxyisilanes and water, a solution of ethoxyisilanes/water is quickly separated into two phases. Instead, a large amount of alcohol has been used as a reaction medium to dissolve ethoxyisilanes in water to prevent phase separation of the ethoxyisilanes/water solution. In contrast to ethoxyisilanes, it is important to note that methoxyisilanes do not require alcohol to be dissolved in water due to the self-hydrolysis of methoxyisilanes into organosilanetriols. The unique self-hydrolysis phenomenon of methoxyisilanes depends on its molecular structure and organofunctional groups.

A methoxyisilane molecule has three easily hydrolyzable methoxy groups suitable for changing from methoxy groups to hydroxyl groups, and the rate of hydrolysis significantly greater than ethoxyisilane molecule. In addition, methoxyisilanes liberate methanol as a byproduct during the hydrolysis reaction.²⁶ The generated methanol helps the methoxyisilanes precursor to be fully dissolved into water. Subsequently, methoxyisilanes are polymerized in the alcohol-free sol–gel system, and the

traditional cosolvent concept proposed in the Stober–Fink–Bohn (SFB) method is unnecessary.²⁷ Under basic conditions, the hydrolysis of methoxy groups usually takes place in a stepwise manner.

As seen from DLS and SEM data in Table 2, the particle size difference among various FPSQ particles obtained using low and high catalyst concentrations were smaller and larger, respectively. The results confirmed that carbon-bonded substituents can have profound effects on particle size and rate of hydrolysis. Surfactants were used to disperse and stabilize hydrophobic functional methoxyisilanes in aqueous medium. When the surfactants were added into water, the homogeneous solution was converted into a heterogeneous solution including (functional) methoxyisilane droplets of various sizes. As a result, particles with broad size distribution resulted in the heterogeneous solution after complete hydrolysis,²⁸ which might be another reason for the polydispersity.

Additionally, various sizes of FPSQ particles can be selectively obtained at different catalyst concentration levels, and polydispersity increased with an increase in catalyst concentration. As the catalyst concentration increased, the reaction rate also increased so that more nuclei are formed. Thus, when the catalyst concentration was increased, particle growth was limited and the average particle size was decreased. It was determined that the size and size distribution of FPSQ particles can be controlled by the selection of surfactant concentration, catalyst concentration, organomethoxyisilane ratios, and functionality.

Elemental Analysis. The organic content percentages obtained from the elemental analyses were in reasonable agreement with the theoretical values for all FPSQ materials prepared using the alcohol-free hydrolytic sol–gel approach, as shown in Table 3. The results confirmed the successful preparation of copolymerized FPSQs by a hydrolytic co-condensation of organomethoxyisilanes.

FT-IR Spectroscopy. The presence of characteristic bands of FPQs in the FT-IR spectra (see Figure 6) confirmed the formation of Si–O–Si bonds and the retention of Si–C linkages during the hydrolytic co-condensation reactions.²⁹ The silsesquioxanes exhibited well-defined absorptions at ca. 1405–1415 cm^{-1} , characteristic of symmetric deformations in Si–R groups. CH and Si–C stretching vibrations were observed at ca. 2900–3080 and 775–782 cm^{-1} , respectively. The presence of Si–O–Si linkages was further supported by strong absorptions at 1130 cm^{-1} (stretching) and 1030 cm^{-1} (flexing) and distinct vibrations at ca. 430–500 cm^{-1} (bending). The C=C double bond absorption band was seen in the IR spectrum of MA-PSQ3 and V-PSQ2 at 1705 cm^{-1} , but on the other hand, the C=O vibration band at 1630 cm^{-1} was obscured by the strong absorptions characteristic of Si–O–Si bonds. The IR spectra show a well-defined C–H absorption of Si–CH₃ at 1278 cm^{-1} .

NMR Spectroscopy. Solid-state ¹³C and ²⁹Si NMR spectroscopies are powerful methods for characterizing the chemical structure of the powders prepared from organoalkoxyisilanes.⁷ Solid-state MAS ²⁹Si NMR spectroscopy provides quantitative information about the condensation reaction, and solid-state ¹³C NMR spectroscopy is particularly useful in determining the extent of the hydrolysis reaction. Solid-state MAS ²⁹Si NMR spectra of the FPSQ powders are shown in Figure 7a. The peaks at –80.09 and –71.25 ppm in ²⁹Si NMR spectra of the FPSQ powders were assigned to fully condensed T³ and T² species, respectively. T¹ peaks were too small to be analyzed in the spectra. The formation of T¹ and T⁰ species was insignificant, suggesting that no unreacted organically modified precursor was present.²⁰

Figure 7b shows the solid-state ¹³C CP/MAS NMR spectra of FPSQ powders. The observation of two resonance peaks at

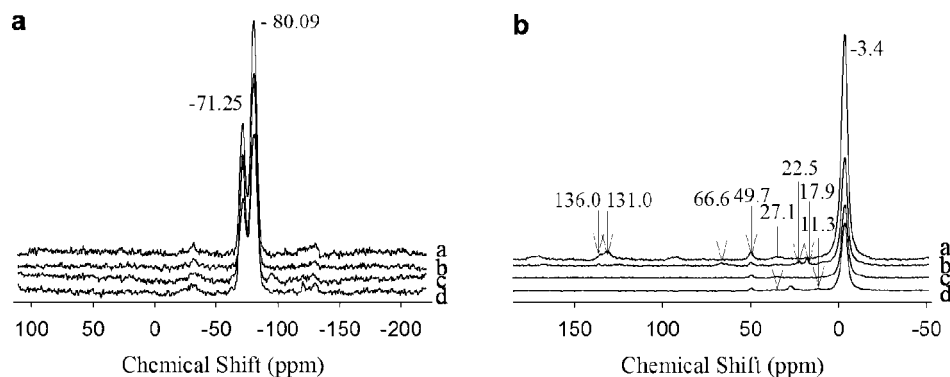


Figure 7. (a) ^{29}Si CP MAS NMR spectra: a, M-PSQ1; b, MA-PSQ3; c, V-PSQ2; d, MP-PSQ6. (b) ^{13}C CP MAS NMR spectra: a, V-PSQ2; b, MA-PSQ3; c, M-PSQ1; d, MP-PSQ6 of FPSQs.

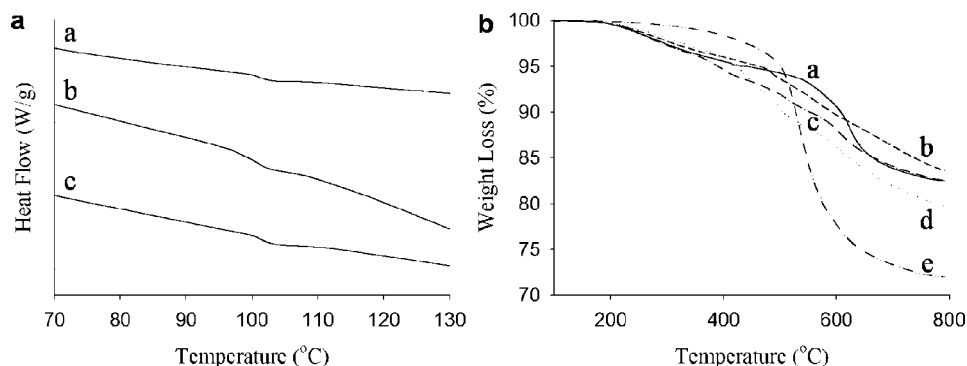


Figure 8. (a) DSC curves: a, M-PSQ1; b, MA-PSQ3; c, MP-PSQ6. (b) TGA curves: a, M-PSQ1; b, V-PSQ2; c, MP-PSQ6; d, MA-PSQ3; e, A-PSQ2 of FPSQs.

Table 4. Surface Area Analysis for Methylsilsesquioxanes

material	BET surface area ($S_{\text{BET}}/\text{m}^2 \text{ g}^{-1}$)	total pore volume ($V_{\text{p}}/\text{cm}^3 \text{ g}^{-1}$)	micropore volume ($V_{\text{mp}}/\text{cm}^3 \text{ g}^{-1}$)	av pore diameter (D/nm)	porosity, φ (%)
M-PSQ1	2.0	0.005	0.00	10.0	1.10
M-PSQ2	84.3	0.318	0.00	15.0	41.10

131 and 136 ppm in the ^{13}C CP/MAS NMR spectra revealed the presence of vinyl functional groups, as seen in Figure 7b-(a). The intense peak at -3.4 ppm is due to the carbon signal from the methyl group of MTMS. The resonances (see Figure 7b-(b)) at near 66.6, 22.5, 17.9, and 11.3 ppm were assigned to unreacted methacryloxypropyl carbon atoms of MAPTMS.²⁰ The NMR curve (see Figure 7b-(d)) showed signals at 27.1 ppm (C1, C2) in addition to a slightly shifted downfield $\text{CH}_2\text{-(Si)}$ (C3) signal at 11.3 ppm for the $\text{-(CH}_2\text{)}_3\text{SH}$ moiety. The ^{13}C CP/MAS NMR spectra of the products were consistent with the expected structures, although in some cases a small signal at 49–50 ppm was attributed to traces of emulsifier remaining in the product. The NMR data were also consistent with the formation of relatively highly condensed FPSQ networks.

Thermal Properties. DSC analyses were carried out for the representative FPSQs, and the curves are presented in Figure 8a. The glass transition temperatures of M-PSQ1, MP-PSQ6, and MA-PSQ3 were observed at 101, 100, and 99 $^\circ\text{C}$, respectively. Therefore, the T_g of cohydrolyzates decreased marginally compared to M-PSQ1, which may be due to the effect of small amount organic functional silane comonomer.

The thermal stability of the FPSQs was investigated using TGA. The influence of the functional methoxysilane on the different cohydrolyzates in comparison with M-PSQ1 was analyzed by interpreting the decomposition temperature. Figure 8b shows TGA traces of FPSQs, and the obtained results are summarized in Table 3. The thermal reduction of siloxane network had a maximum velocity in the 400–700 $^\circ\text{C}$ range,

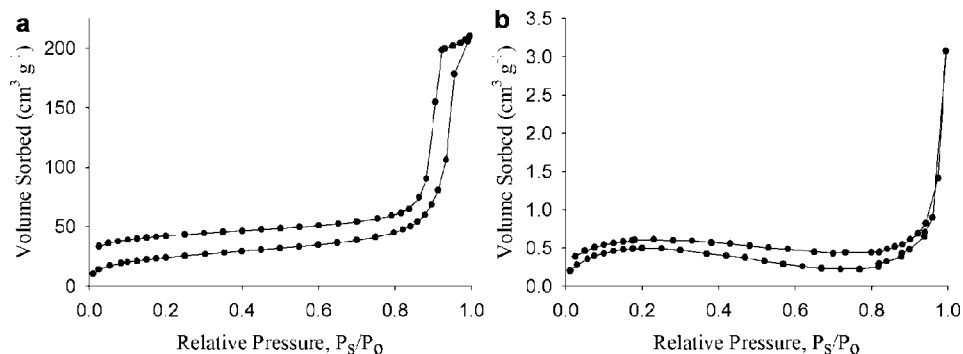


Figure 9. Nitrogen adsorption–desorption isotherm for methylsilsesquioxanes: (a) M-PSQ2 and (b) M-PSQ1.

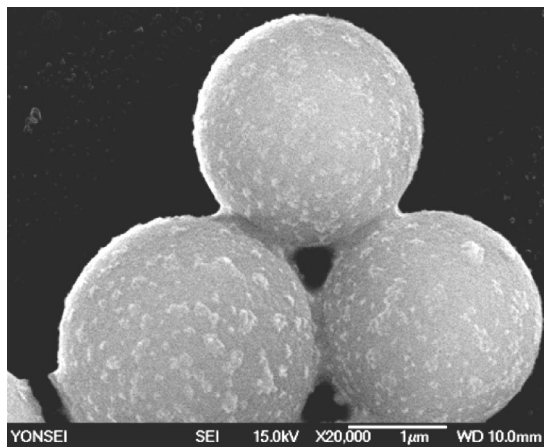


Figure 10. A representative SEM image to confirm the interaction between mercapto FPSQ particles and gold ions.

arising from the loss of organic moieties groups.¹⁹ As expected, M-PSQ1 and V-PSQ2 showed the highest decomposition temperature. The thermal decomposition temperatures of the FPSQs, at 15% weight loss, increased in the order A-PSQ2 < MA-PSQ3 < MP-PSQ6 < M-PSQ1 < V-PSQ2. The result was ascribed to the higher thermal stability of the methyl and vinyl groups compared to the organic functional groups. The rapid weight loss of A-PSQ2 appeared to be mainly due to the decomposition of aminopropyl groups. The higher the inorganic or the lower the organic contents were of the FPSQs, then the thermal stability was found higher.

Surface Area and Porosity Analysis. The specific surface areas, average pore diameter and porosity of the representative nano and micro M-PSQs particles were evaluated using the BET method and the results are given in Table 4. Specific surface areas of the micro M-PSQ1 and nano M-PSQ2 particles that were evaluated through BET equation were 2.0 and 84.3 m²/g, respectively. The average pore diameter of the micro (M-PSQ1) and nano (M-PSQ2) particles were 10 and 15 nm and porosity was 1.1 and 41.1%, respectively. The relatively small S_{BET} values were due to complete condensation of FPSQs. The results were consistent with those of the SEM images. The adsorption-desorption isotherms exhibited (see Figure 9) indicated that the FPSQ spheres were fairly typical of mesoporous solids with pore diameters in the range 2–50 nm (type IV isotherm).^{30,31}

FPSQ Particles and Metal Ions Interactions. The interaction between gold ions and the representative mercapto FPSQ particles sample was studied by heating mixtures of aqueous solutions of hydrogen tetrachloroaurate(III) trihydrate and the FPSQ particles at 70 °C. Evidently, the SEM images of microparticles recovered from such mixtures showed the presence of gold nanoparticles on the surface of the mercapto FPSQ microparticles, as shown in Figure 10. It was found that mercapto groups were responsible for the formation and fixation of gold nanoparticles in this study. The study confirmed that mercapto groups in FPSQ were very useful for the preparation of metal/polymer (nano)composite particles without the aid of any other reductant or stabilizer. The concentration of the metal particles on the final metal/FPSQs nanocomposite particles was controlled by varying the composition or controlling the functional groups of the cohydrolyzate (MTMS/MPTMS ratio).

Conclusions

Hydrolytic co-condensation was used to synthesize a series of organic FPSQ nano/micro particles of narrow size distributions using MTMS as main precursor in the presence of base

catalyst and surfactant. The process is a one-step co-condensation synthetic route where the functionalities and diameters of the particles can be controlled by the organosilane ratio and catalyst concentration, respectively. Self-hydrolysis of methoxysilanes in the presence of base catalyst accounted for preparation of nano/micro particles of narrow size distributions. The results of elemental analysis, solid-state NMR spectroscopy, and FT-IR analysis confirmed the co-condensation between alkoxysilanes and the formation of Si–O–Si bonds during the hydrolysis and condensation reactions. Thermal analysis confirmed that T_g of the silsesquioxanes found were near 100 °C while initial decomposition occurred at 400 °C and above. FPSQ particle morphology and the interaction between FPSQ particles and metal ions were confirmed by SEM studies. The presence of organic functional groups can be further extended or modified chemically with other organic or inorganic functional materials. The process has the capability for synthesizing diverse organic/inorganic hybrid materials.

Acknowledgment. This work was financially supported by the Ministry of Education and Human Resources Development (MOE), the Ministry of Commerce, Industry and Energy (MOCIE), and the Ministry of Labor (MOLAB) through fostering project of the Laboratory of Excellence. This work was supported by Ministry of Commerce, Industry and Energy (MOCIE), through the project of NGNT (No. 10024146). This work was also supported by the Korea Science and Engineering Foundation (KOSEF) grant funded by the Korea government (MOST) (No. R11-2007-050-02001-0). The authors thank Dr. Thomas P. Schuman, Missouri University of Science and Technology, for his valuable contribution.

References and Notes

- (1) Li, G.; Wang, L.; Ni, H.; Pittman, C. U., Jr. *J. Inorg. Organomet. Polym.* **2002**, *11*, 123–154.
- (2) Harrison, P. G. *J. Organomet. Chem.* **1997**, *542*, 141–183.
- (3) Baney, R. H.; Itoh, M.; Sakakibara, A.; Suzuki, T. *Chem. Rev.* **1995**, *95*, 1409–30.
- (4) Voronkov, M. G.; Lavrent'yev, V. I. *Top. Curr. Chem.* **1982**, *102*, 199–236.
- (5) Shea, K. J.; Loy, D. A. *Chem. Mater.* **2001**, *13*, 3306–3319.
- (6) Stoeber, W.; Fink, A.; Bohn, E. *J. Colloid Interface Sci.* **1968**, *26*, 62–9.
- (7) Van Blaaderen, A.; Vrij, A. *J. Colloid Interface Sci.* **1993**, *156*, 1–18.
- (8) Suratwala, T. I.; Hanna, M. L.; Miller, E. L.; Whitman, P. K.; Thomas, I. M.; Ehrmann, P. R.; Maxwell, R. S.; Burnham, A. K. *J. Non-Cryst. Solids* **2003**, *316*, 349–363.
- (9) Hatakeyama, F.; Kanzaki, S. *J. Am. Ceram. Soc.* **1990**, *73*, 2107–10.
- (10) Yacoub-George, E.; Bratz, E.; Tilscher, H. *J. Non-Cryst. Solids* **1994**, *167*, 9–15.
- (11) Silva, C. R.; Airoidi, C. *J. Colloid Interface Sci.* **1997**, *195*, 381–387.
- (12) Reynolds, K. J.; Colon, L. A. *J. Liq. Chromatogr. Relat. Technol.* **2000**, *23*, 161–173.
- (13) Etienne, M.; Lebeau, B.; Walcarius, A. *New J. Chem.* **2002**, *26*, 384–386.
- (14) Yin, R.; Ottenbrite, R. M.; Siddiqui, J. A. *Polym. Prepr.* **1995**, *36*, 265–6.
- (15) Choi, J. Y.; Kim, C. H.; Kim, D. K. *J. Am. Ceram. Soc.* **1998**, *81*, 1184–1188.
- (16) Kim, Y. B.; Kim, Y.-A.; Yoon, K.-S. *Macromol. Rapid Commun.* **2006**, *27*, 1247–1253.
- (17) Liu, S.; Lang, X.; Ye, H.; Zhang, S.; Zhao, J. *Eur. Polym. J.* **2005**, *41*, 996–1001.
- (18) Noda, I.; Isikawa, M.; Yamawaki, M.; Sasaki, Y. *Inorg. Chim. Acta* **1997**, *263*, 149–152.
- (19) Arkhireeva, A.; Hay, J. N.; Oware, W. *J. Non-Cryst. Solids* **2005**, *351*, 1688–1695.
- (20) Arkhireeva, A.; Hay, J. N. *J. Mater. Chem.* **2003**, *13*, 3122–3127.
- (21) Lee, Y.-G.; Park, J.-H.; Oh, C.; Oh, S.-G.; Kim, Y. C. *Langmuir* **2007**, *23*, 10875–10878.
- (22) Brunel, D.; Cauvel, A.; Fajula, F.; DiRenzo, F. *Stud. Surf. Sci. Catal.* **1995**, *97*, 173–80.
- (23) Harreld, J. H.; Su, K.; Katsoulis, D. E.; Suto, M.; Stucky, G. D. *Chem. Mater.* **2002**, *14*, 1174–1182.
- (24) Shimizu, I.; Yoshino, A.; Okabayashi, H.; Nishio, E.; O'Connor, C. J. *J. Chem. Soc., Faraday Trans.* **1997**, *93*, 1971–1979.

- (25) Beari, F.; Brand, M.; Jenkner, P.; Lehnert, R.; Metternich, H. J.; Monkiewicz, J.; Siesler, H. W. *J. Organomet. Chem.* **2001**, 625, 208–216.
- (26) Iler, R. K. *The Chemistry of Silica*; John Wiley & Sons: New York, 1979; p 892.
- (27) Avnir, D.; Kaufman, V. R. *J. Non-Cryst. Solids* **1987**, 92, 180–2.
- (28) Lee, Y.-G.; Oh, C.; Yoo, S.-K.; Koo, S.-M.; Oh, S.-G. *Microporous Mesoporous Mater.* **2005**, 86, 134–144.
- (29) Anderson, D. R. In *Analysis of Silicones*; Wiley-Interscience: New York, 1974; Vol. 41, pp 247–86.
- (30) Gregg, S. J.; Sing, K. S. W. *Adsorption, Surface Area and Porosity*, 2nd ed.; Academic Press: London, 1982; p 303.
- (31) Leofanti, G.; Padovan, M.; Tozzola, G.; Venturelli, B. *Catal. Today* **1998**, 41, 207–219.

MA8003345